Lackner *et al.*
European Transport Research Review (2023) 15:22
https://doi.org/10.1186/s12544-023-00595-0

European Transport
Research Review

ORIGINAL PAPER **Open Access**

Investigations on tram-pedestrian impacts by application of virtual testing with human body models

Christian Lackner[1*], Philipp Heinzl[1], Christoph Leo[2] and Corina Klug[2]

Abstract

Background In Austria around 100 trams are involved in accidents with pedestrians every year. Since the service lives of trams are very high, the probabilities are also high that each tram on the network will be involved in an accident of this kind at least once, highlighting the need of protective designs of tram fronts. However, due to lack of studies in this area, this is still a challenging task.

Purpose The aim of this study is to show the applicability and the usability of virtual testing involving HBMs in tram front design studies to improve passive safety in general.

Methodology In this study, the impact of pedestrians with a tram was investigated using a generic tram front model in a basic version and a conceptually improved version, respectively, and detailed finite element human body models (HBM). To consider gender-differences and to avoid designs that unintentionally favour only particular groups of the population, the study simulations were carried out with a male and a female 50th percentile finite element human body model (VIVA+). The risk for head, chest, femur and tibia injuries were analysed as the simulation result, since these body areas were identified based on field data to be most relevant in accidents involving pedestrians and trams. Collision scenarios are evaluated for a wide parameter variation in impact location and speed, respectively.

Findings The results show a reduction in head injury risk for both the female and the male HBM at different speeds and impact locations for impact with the enhanced version of the tram front. Depending on the gender of the HBM, the considered improvement shows different effects for each body region, with a greater reduction in the likelihood of head injury for the female model, and a greater reduction in the likelihood of thoracic injury for the male model. These differences are due to the considered anthropomorphic variations. A reduction for the risk of femur injuries can be achieved in all cases using the modified tram front. The study showcases the application of detailed human body models for tram pedestrian impact analyses in the context of pedestrian safety and in particular for tram front improvements. It was shown that even a minor modification of the tram front with softer front skirt attachments leads to remarkable benefits with respect to injury criteria in all investigated crash scenarios. The presented research goes beyond current technical recommendations and shows the benefit of virtual testing including HBMs and considering a wide variety of impact speeds, anthropometries and injury assessments, respectively.

Keywords Accident parameter, Injuries, Injury severity, Pedestrian, Public transport, Tram

---

*Correspondence:
Christian Lackner
lackner.christian@siemens.com
Full list of author information is available at the end of the article

1 Introduction

Tram transport is gaining more importance across Europe again but also safety concerns are raised because of the poor manoeuvrability and the long braking distances of trams in general [25]. There are even tram stops with shared space between pedestrians, trams and cars. To think about prevention of accidents with pedestrians in the first place is rather obvious. This can be achieved e.g. by improving the visibility of the tram itself, fences between the tram tracks and the pedestrian area, separate signal phases for trams and pedestrians, road markings indicating the area used by the tram or by increasing the operator's field of view by the tram cab's design.

The risk of a pedestrian accident involving at least one tram is about 1.4 per million kilometres travelled [18]. Most of these accidents result in minor injuries (Accident risk of 0.9), although fatal and severe injuries are also present since the risk for these is about 0.5 per million km travelled. The estimated median speed leading to minor injuries is about 28 kph and 36 kph to severe injuries, respectively [18]. The theoretical maximum speed of tram vehicles is about 70 kph [28], but this speed is usually not reached under typical urban conditions [12] due to curves, poor track conditions or short distances between stops, traffic lights etc. The average tram travel speed in the City of Vienna for example, is about 15 kph [35].

Although tram-pedestrian impacts are relatively common, only a few studies have been conducted on these. Compared to the automotive sector, hardly any pedestrian protection innovations were introduced in tram development in the past. One reason for this is the lack of a standardization in tram-pedestrian safety assessments. In this context, the trams' front mask is of particular interest. Today's best practice for tram pedestrian protection is to follow the geometry-based tram front design guidelines of CEN/TR 17420 [32]. Above all, these design guidelines guarantee a certain overall curved tram front to establish reasonable lateral deflection of the pedestrian and a maximum steepness so that pedestrian are thrown back upwards. This technical report [32] also includes some guidelines on how to verify the passive safety of trams by using numerical simulations with anthropomorphic test devices (ATD). The accident scenario of a pedestrian against a tram front with a constant speed of 20 kph at 7.5% and 25% tram width must be evaluated if the geometric recommendations are not fulfilled by the vehicle front. The evaluation must be performed with two ATDs of different sizes, a 50th percentile male and a 6-year-old child. The shape, mass, and stiffness of the impact zones must be modelled with sufficient accuracy with respect to the tram under investigation. Passive safety requirements are met if both of the following criteria are met:

- HIC_{15} for the head impact at both impact locations with both ATD's below 1000 each.
- Lateral deflection of the ATD of at least 800 mm.

One remarkable study on various tram types across Swiss cities focusses on HIC and head impact velocity at speeds up to 30 kph using standing Hybrid III dummies as pedestrian models (6-year-old and 50th percentile pedestrian) simulated in Madymo [34]. This study shows HIC values beyond 1000 for most impacts already at 20 kph during the primary impact, but even higher HIC values for the secondary impacts onto the ground. The values for HIC were lowered with an increased gap between front skirts and windscreen. Recommendations were made such as avoiding protruding parts and sharp edges, covering the A-pillars and increasing the horizontal distance between the windscreen and the front skirts of the tram, which led to decreases of HIC values in their study.

Statistical data related to tram-pedestrian accidents [18] shows the affected body regions also broken down by gender. Based on the Swedish Accident Database STRADA, it is shown that tram-pedestrian accidents mainly lead to head and thoracic injuries but also to high risks for lower extremity injuries. Male pedestrians have a slightly higher head injury risk whereas the females' risk of suffering injuries to the abdomen or lower extremities is about twice compared to the males. Based on these findings this new study is particularly on the comparison of injury risks in tram accidents between female and male pedestrians.

Human body models (HBMs) are widely used for the analysis of injury mechanisms and optimisation of vehicle fronts in the automotive industry [10, 15, 20, 29, 33]. These are already used in Euro NCAP (European New Car Assessment Programme) for the assessment of deployable systems, to determine head impact timing and location [16]. HBMs are a virtual geometric and mechanical representation of the human body. Finite Element HBMs feature a high level of anatomical details of the human body. They are validated over a wide range of different loadcases and unlike the situation with ATDs also tissue-based injury metrics can be analysed in addition to kinematics.

Although HBMs also have the advantage of enabling consideration for anthropometric variations, the average male anthropometry alone is still only considered in most of the studies. This problem was further investigated in the VIRTUAL project and addressed by developing an HBM which was designed to enable morphing in good mesh quality. These are known as VIVA + models

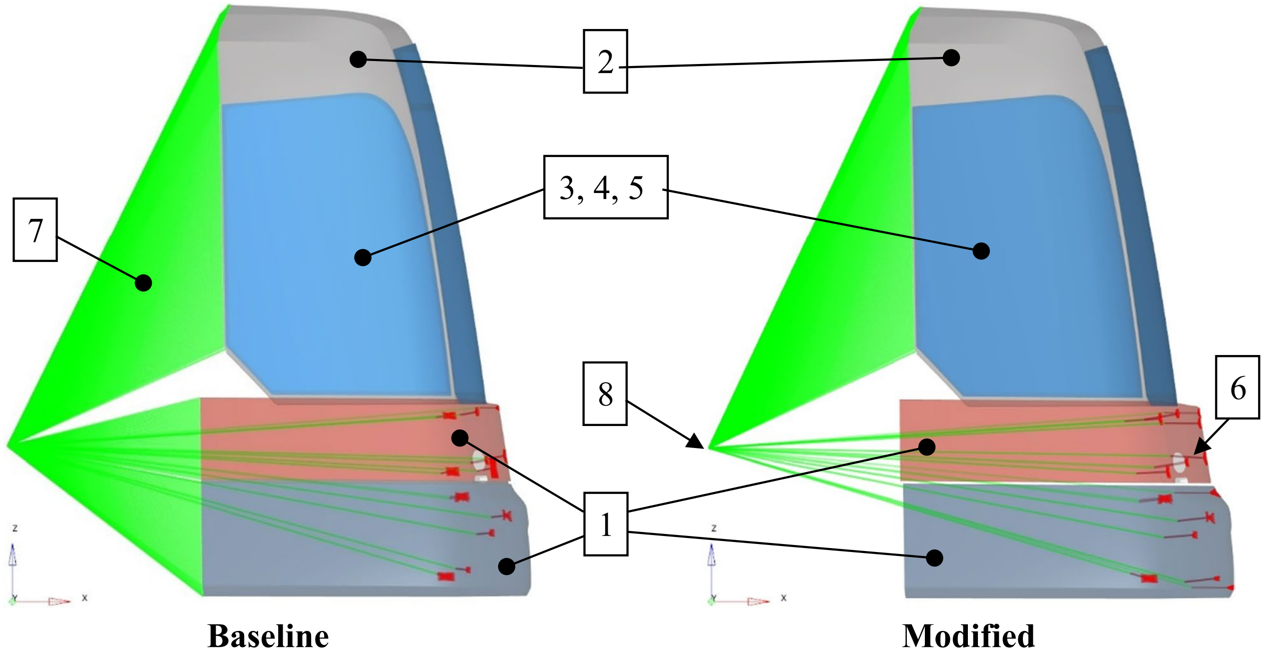

Fig. 1 Visualization of both, baseline and modified tram fronts

Table 1 Element type, properties and material cards of generic tram components for simulations in LS-DYNA

Nr	Component	Elem. type	Properties	Material model in LS-DYNA [22]
1	Front skirts	Shell	4.00 mm	*MAT_001/*MAT_ELASTIC
2	Cab Frame	Shell	6.00 mm	*MAT_001/*MAT_ELASTIC
3	Inner glass sheet	Shell	3.00 mm	*MAT_280/*MAT_GLASS
4	Interlayer	Solid	0.76 mm	*MAT_181/ *MAT_SIMPLIFIED_RUBBER
5	Outer glass sheet	Shell	4.00 mm	*MAT_280/*MAT_GLASS
6	Brackets	Beams	Figure 1	*MAT_119/ *MAT_GENERAL_NONLINEAR
7	Rigid Body	Constr._Rigid_Bodies	–	–
8	Mass	Element_Mass	20,000 kg	–

and they are available as average male and also as average female versions. Passive safety measures of vehicles can thus be assessed with a 50th percentile male and 50th percentile female human for subsequently improving its safety equally for both genders [14, 21].

This paper examines injury mechanisms considering gender differences using virtual testing, as literature on this topic is not yet available. Virtual testing leads to a direct injury risk assessments and comparisons, respectively, for different body regions, -dimensions and genders. This work describes a novel methodology that can lead to future tram fronts designs with considerably increased passive safety with regard to pedestrian accidents.

2 Materials and methods

2.1 Generic tram

To test different tram front designs a simplified generic tram front finite element model used for simulations with LS-DYNA R12.1 was developed, which is easily adjustable in its stiffness and is shown in Fig. 1 with transparent surface elements. The shape of the generic tram complies with the geometric recommendations of CEN/TR 17420 [32]. The components of the generic tram front are listed in Table 1. The front skirts of the tram are modelled with *MAT_001/**MAT_ELASTIC* with some basic parameters, e.g. a Young's modulus of 25 kN/mm^2, a Poisson's ratio of 0.25 and a density of $2.0e^{-6}$ kg/mm^3, to reproduce the behaviour of glass reinforced plastic (GRP) material which is expected to

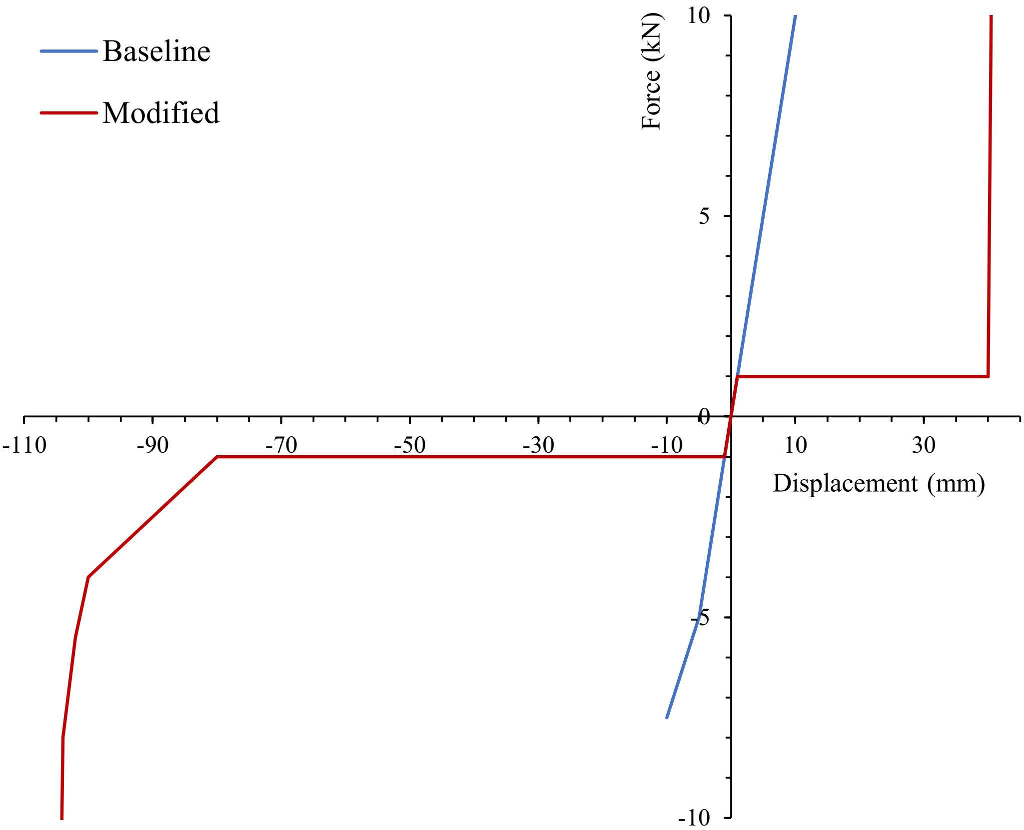

Fig. 2 Diagram of nonlinear force–deflection curve of beam elements (simplification of brackets for front skirts) for baseline and modified tram front version

behave purely elastically in case of pedestrian impacts. The windscreen is modelled in greater detail, as most of the injuries in tram-pedestrian impacts involve the head [18] which often leads to breaking windscreens. It is made up of three layers, two layers of shell elements and one layer of solid elements in between. The shell elements are set to material type *MAT_280/*MAT_GLASS*, which is a smeared fixed crack model combined with Rankine failure criteria. A Young's modulus of 73 kN/mm^2, a Poisson's ratio of 0.2 and a density of 2.5e^{-6} kg/mm^3 are used for the panes of glass. For this model, additional force–displacement curves from an empirical study [13] were used to calibrate the remaining material parameters in a separate simulation setup. The solid elements were modelled with *MAT_181/**MAT_SIMPLIFIED_RUBBER/FOAM*, which considers stress–strain curves at six different strain rates from 0.001 s^{-1} up to 1360 s^{-1} taken from Kuntsche [17] and Zhang et al. [37] and a material density of 1.081e^{-6} kg/mm^3. Failure modes of laminated glass are strongly velocity dependent [23], and the relevant critical impact velocity for failure of glass is likely not reached at a head impact velocity below 20 kph. Since no tram windscreen glass data is available in any more detail yet the impact speed range of 25–35 kph is also run with a pure elastic glass behaviour to also cover possible negative effects due to a non-braking windscreen in the head impact (relative) velocity range below 20 kph. The windscreen is mounted with a tied contact formulation to the cab's frame, which is also modelled as elastic GRP material, exactly like the front skirts, but with thicker shell elements. In the basic tram model, the upper and lower front skirts are interconnected, but in the modified version they are separated so they can move independently from each other to provide a better support for the struck pedestrian.

Between the vehicle body (lumped mass of 20,000 kg) and the brackets, which are modelled as beam elements, there is a constrained rigid body, which is additionally connected to the rear of the tram. Either the stiffness or softness, of the vehicle's foremost front is adjustable via these beam elements that connect the vehicle with the front skirt panels. Their overall behaviour is described through force vs. deflection characteristics applied to the translational degrees of freedom

Table 2 Injury prediction of different body regions

Criteria	Based on	Sources
HIC	Resultant Head CoG accelerations filtered with CFC1000	Schmitt et al. [26]
DAMAGE MPS	DAMAGE Implementation in Dynasaur using head rotation sensors implemented in VIVA + definition files, filtered with CFC60	Gabler et al. [11] Wu et al. [36] Euro NCAP [8]
Risk of fractured ribs	Risk per rib determined based on maximum strain per rib Combined to overall risk of fractured ribs using probabilistic method	Larsson et al. [19] Forman et al. [9]
Proximal femur fracture risk	Risk based on MPS99 using risk curves calibrated for VIVA + model	Schubert et al. [27]
Femur shaft fracture risk	Risk based on MPS99 using risk curves calibrated for VIVA + model	Schubert et al. [27]
Tibia shaft fracture risk	Risk based on MPS99 using risk curves calibrated for VIVA + model	Developed in WP2 of VIRTUAL (unpublished)

(DOFs) along the beams' local s-, t- and r- axes. The modified tram front model has its front skirts mounted to the frame via beams that are very soft for the first 80 mm of deflection and provide a progressive stiffness increase to a total possible stroke of 105 mm whereas the standard model's beam connections are modelled quite stiff, please see Fig. 2.

2.2 Pedestrian models

For the in-crash simulations, the VIVA + 50F and 50 M models [14] with revision 0.3.2.a were used with the posture in accordance with the Euro NCAP Technical Bulletin TB024 [6]. The pedestrian model was also fitted with a pair of shoes, also in accordance with the Euro NCAP Technical Bulletin TB024 [6]. The material properties of the VIVA + shoes are based on Cho et al. [3]. The baseline shoe geometry is based on freely available geometry data.[1] Each shoe consists of the following parts: Fabric outer, Fabric inner, Sole inner, Sole mid and Sole outer.

2.3 Injury assessment

The focus of this study is on the head, thoracic, hip, femur and tibia injuries and also on the overall kinematics of the human body model after the impact.

Translational and rotational accelerations are of high relevance in particular for the head injury assessment both [30]: the head impact criterion (HIC) requires translational accelerations and is more related to skull fractures [26], while the diffuse axonal, multi-axis, general evaluation metric (DAMAGE) criterion [24] uses rotational accelerations, respectively. The results for DAMAGE additionally are classified into expected injury levels according to the well-known abbreviated injury scale (AIS) [1] scheme: minor (AIS1), moderate (AIS2) and severe to fatal (AIS4+) are evaluated separately.

Thoracic injuries are evaluated with respect to rib fracture probability by application of a strain-based prediction model. The injury risk curve developed by Larsson et al. [19] was used for the injury risk of each individual rib. This injury risk curve is based on the maximum principle strain. The evaluated risk for each individual Rib can then be used to calculate the overall risk of fractured ribs with the help of the probabilistic method introduced by Forman et al. [9]. I.e., the number of ribs that are likely to be broken is available for each load case by this means.

The different injury prediction models for each body region that were investigated in this study are listed and referenced in Table 2.

The total lateral deflection of the HBM after impact with the tram front is calculated by assuming a parabolic trajectory with the centre of gravity (CoG) of the HBM as its origin. The initial conditions of this trajectory are taken from the kinematic data 15 ms after the contact force between the HBM and the tram becomes zero. As suggested in [32], the criterion is a lateral deflection of at least 800 mm from the point of impact (with an impact velocity of 20 kph) to ensure that no body parts can subsequently be run over by the tram.

The overall injury probability for each body region and collision speed can also be estimated based on accident occurrence probabilities from real world data collected by Lackner et al. [18]. The overall injury risk can be calculated by summing up the injury probabilities of each collision speed multiplied by the respective occurrence probability taken from Additional file 1: Table S1. Finally, the resulting overall injury risks per body region can be used for instance as input for the cost–benefit-analysis developed in Project VIRTUAL [2].

2.4 Simulation setup

The simulations were run with LS-Dyna Version 12.1 mpp single precision. Simulation control and database handling were taken over unchanged from the

---

[1] https://free3d.com

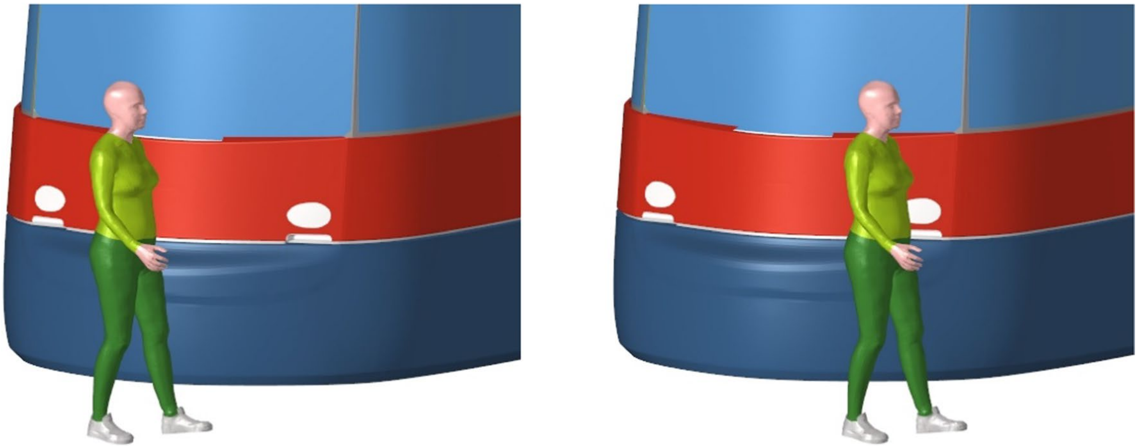

Fig. 3 VIVA + 50F model in front of generic tram baseline model at 0% (left) and 25% (right) tram width

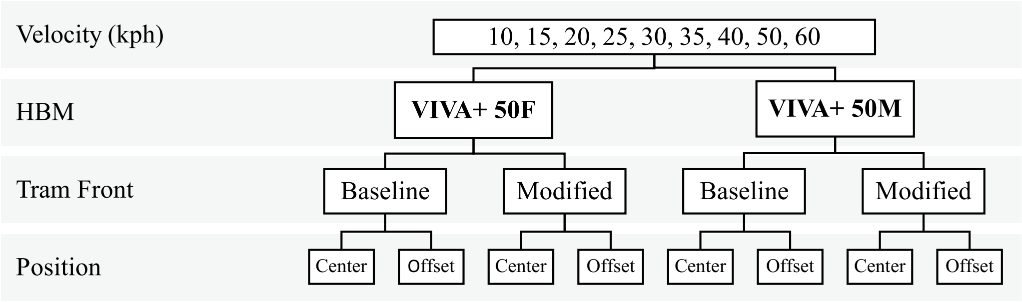

Fig. 4 Simulation Matrix

VIVA + model [14]. For the rearmost nodes, including the point mass of the tram, all degrees of freedom except the x-direction (direction of movement of the tram) are locked. All nodes of the generic tram are defined with an initial velocity depending on the simulated case. Statistical accident data analysis leads to a median speed for severe injuries of about 36 kph [18], therefore initial impact velocities are chosen as follows: 10, 15, 20, 25, 30, 35, 40, 50 and 60 kph.

For the HBM no initial velocity is defined. Gravity is considered for the whole simulation setup, as well as a rigid floor 5 mm lower than the lowest node of the HBM. The HBMs are positioned in walking position as defined in TB024 [7] with the left shoulder facing to the vehicle such as crossing laterally in front of the tram. There are two impact positions defined with respect to the tram width: in the middle of the tram front (0% of the tram width) and an offset of 25% of the tram width in positive y direction (please see Fig. 3), respectively. For both positions, separate simulations for the baseline and the improved tram model, with a 50th percentile female and a 50th percentile male model at all initial velocities defined above are conducted (please see Fig. 4). In the following the individual cases are also labelled according to this figure, e.g. B_50M_v20_25% relates to the baseline tram front model hitting the 50th percentile male HBM at 20 kph and 25% lateral offset.

3 Results

The considered impact scenarios are evaluated in the contexts of head injury, rib, femur and tibia fracture probability and lateral deflection of the HBM, respectively. The kinematic trace lines of individual body regions for both, female and male HBM are shown in Fig. 5. A separate colour is chosen for each body region, the female trajectory is drawn with a solid line, the male trajectory with a dashed line. The abbreviations used in the diagram stand for the following body parts: CoG of Head (HE), CoG of C7 and T12 vertebral bodies (C7, T12), the averaged position of left and right centre of acetabulum (AC), the averaged position of CoG of left and

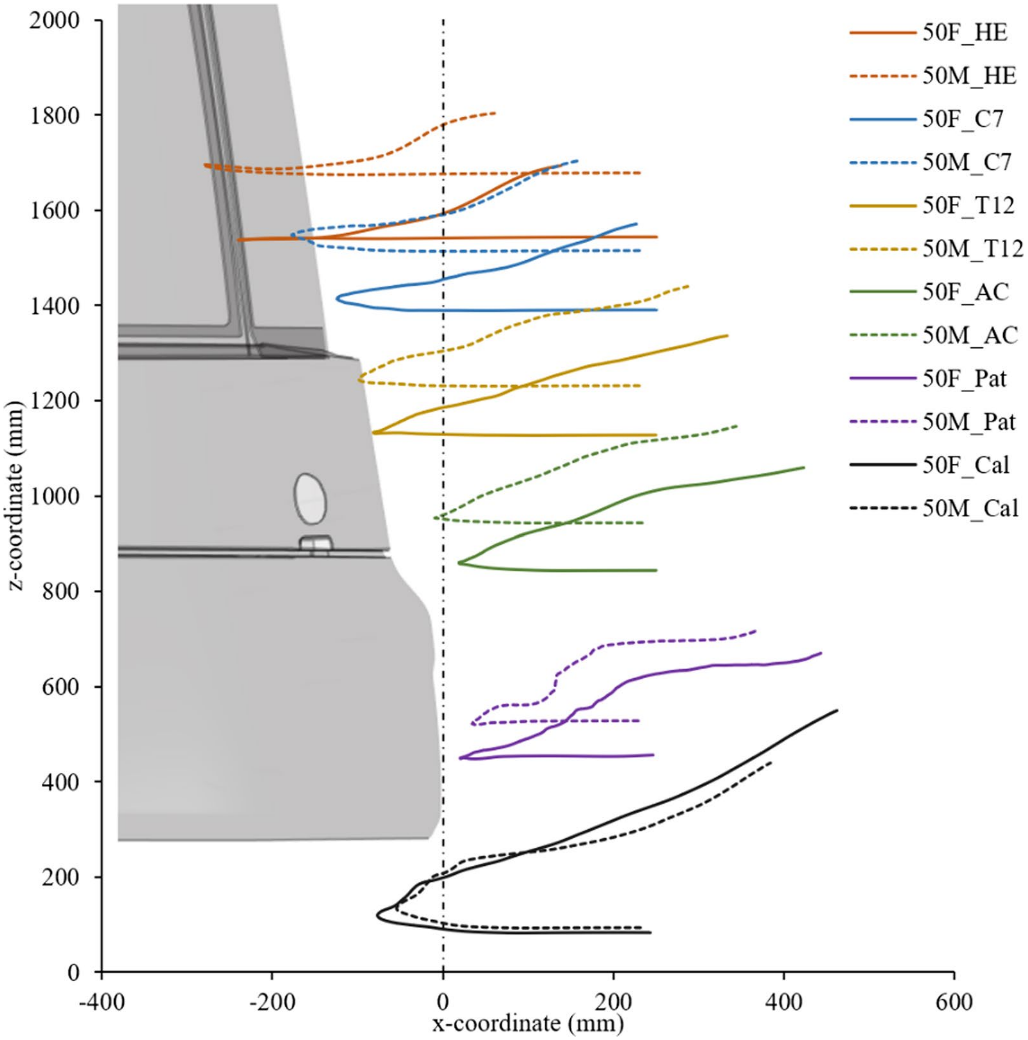

Fig. 5 Kinematics of female and male HBM on baseline tram front with 40 kph speed (centerline)

right patella (Pat) and the averaged position of left and right CoG of calcaneus (Cal).

3.1 Head injury

The evaluations of HIC, DAMAGE (also subdivided into AIS1, AIS2 and AIS4+, respectively) and of the lateral deflection of the HBM in case of the 25% initial lateral offset are provided in the Additional file 1: Figures S1 to S7. All the diagrams offer a direct comparability between the baseline tram front and the softened variant.

In general, the results show low injury indications for impact speeds below 20 kph. Between 20 and 30 kph head injury indications become relevant and from 40 kph on even with respect to severe injuries (ASI4+). Impact speeds of 40 kph and higher always lead to HIC values of level 1000 and above.

The softening of the front skirt attachments leads to a significant reduction of the head impact severity in the centred 50F cases for higher speeds from 40 kph on. The centred 50 M cases generally show significantly lower head injury values which is due to the earlier braking windscreen after the shoulder impact (Additional file 1: Figure S5 and S16).

Figure 6 shows the risk for AIS2 head injuries through assessment of the DAMAGE values for the 25% lateral offset case. Improvements to the tram front can be seen from an impact speed of 20 kph. At impact speeds above 40 kph the injury risk for the 50F HBM is almost 100 percent in both cases the baseline and the modified tram front.

In these cases, it is remarkable that the gender differences are not significantly pronounced and that the head injury indications are generally higher compared to the centred impacts, which is due to the head impact location close to the A-pillar of the tram (Additional file 1: Figure S19 and S20). Additional simulations with a glass

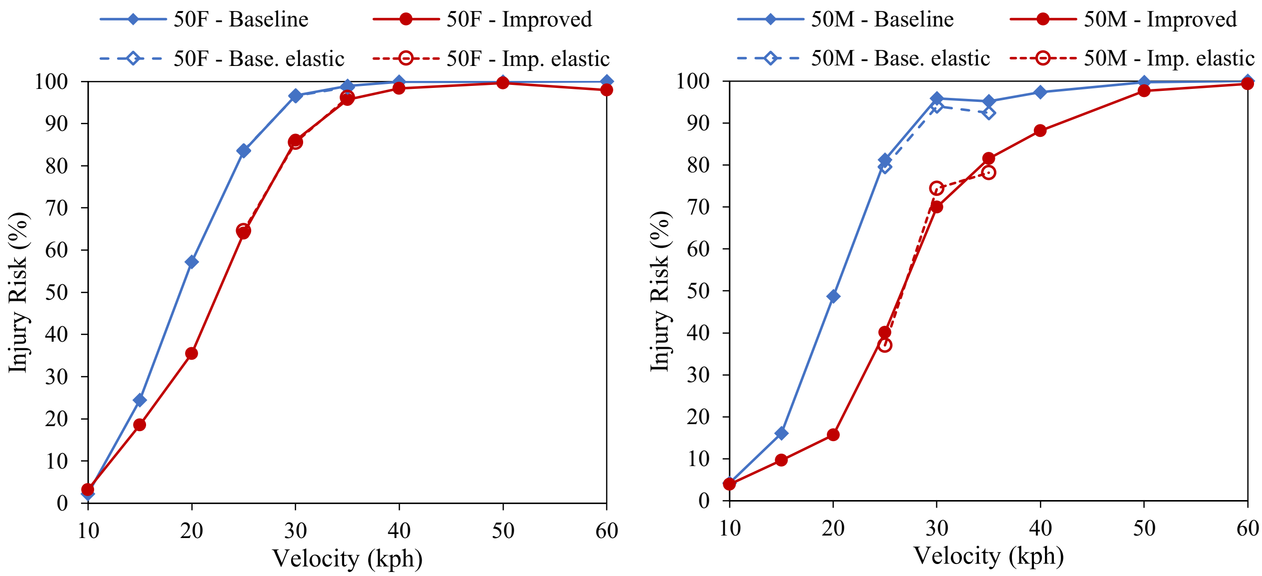

Fig. 6 Injury risk for AIS2 head injury for impact at lateral offset of 25% with female HBM left and male HBM right

model without failure in the velocity range between 25 and 35 kph show very similar results for the 50F, and only in the scenario *_50F_35_0% are the HIC values dramatically higher. For the 50 M, the HIC values are generally higher particularly in the case of a centric impact. The results of the DAMAGE criteria are hardly affected by the change between a glass model with and without failure. Example Additional file 1: Figures S15 to S20 show close-ups of pedestrian against generic tram (glass with failure model) at 50 kph.

3.2 Thorax injury

Table 3 shows the rib fracture probabilities for all considered cases up to an impact speed of 25 kph. The results show a 100% probability for more than three broken ribs for impact speeds above 25 kph, which is considered to result in AIS4+injuries.

For impact speeds up to 25 kph the improved softened tram front can reduce the rib fracture risk in most considered cases. For example, I_50F_20_25% case shows a 25% lower risk of three or more broken ribs compared to the baseline model. In the related scenario with the male HBM, the risk of three or more broken ribs for the male HBM is even decreased by 52%. In the Additional file 1: Figures S21 and S22 show the overall strain distribution of the cortical bones during impact.

3.3 Femur proximity (hip) injury

At lower speeds, the female HBM in particular (see Additional file 1: Figure S9) shows high risks of proximal femur fracture. From tram speeds of 30 km/h on, the baseline version of the tram front consistently shows 100% fracture risk. With the improved version of the tram front the risk of proximal femur fracture is reduced primarily in the speed range between 25 and 40 kph at best by 45%. An equivalent diagram for the male HBM is shown in Additional file 1: Figure S10. The risk for proximal femur fracture is remarkably low for speeds up to 35 kph for the centred impact but increases very sharply for the baseline tram front at higher speeds. In the case of lateral offset impacts at 25%, the baseline model shows an almost linear increase in fracture risk, while the improved tram front apparently caps the fracture risk from 30 kph upwards.

3.4 Femur shaft injury

The situation for femoral shaft fracture is comparable to the proximal femur fracture shown in Additional file 1: Figure S11 for the centred impact of the tram front with the female HBM, while the risk of injury at the 25% lateral offset position is very low for the female HBM.

The fracture risk of the femoral shaft of the male HBM rises very quickly to about 50% already at 25 kph, as shown in Additional file 1: Figure S12, whereas the improved version of the tram front leads to a significant enhancement only at higher speeds from 40 to 50 km/h. For the lateral offset impact at 25% the improved version reduces the injury risk by more than 50% already for speeds from 30 km/h on. At the 25% position and the baseline front the risk increases almost linearly with about 50% risk at a speed between 35 and 40 kph.

Table 3 Rib fracture probabilities

50F	Number of broken ribs	Baseline		Improved	
		Centerline (%)	**Offset (%)**	**Centerline (%)**	**Offset (%)**
10 kph	0	94.9	94.4	87.9	95.2
	1	5.0	5.5	11.6	4.7
	2	0.1	0.1	0.4	0.1
	3+	0.0	0.0	0.0	0.0
15 kph	0	17.8	26.4	18.1	38.1
	1	65.4	40.3	57.7	40.7
	2	15.6	24.2	22.5	17.0
	3+	1.2	9.1	1.7	4.2
20 kph	0	0.1	0.1	0.9	0.5
	1	15.7	0.7	23.7	7.2
	2	35.0	3.8	39.4	21.7
	3+	49.2	95.5	36.1	70.6
25 kph	0	0.0	0.0	0.0	0.0
	1	0.3	0.0	5.8	0.0
	2	3.2	0.0	23.7	0.1
	3+	96.6	100.0	70.5	99.9
50 M	**Number of broken ribs**	**Baseline**		**Improved**	
		Centerline (%)	**Offset (%)**	**Centerline (%)**	**Offset (%)**
10 kph	0	97.2	93.4	98.9	97.7
	1	2.8	6.6	1.1	2.3
	2	0.0	0.0	0.0	0.0
	3+	0.0	0.0	0.0	0.0
15 kph	0	82.2	40.5	81.1	41.9
	1	16.6	43.8	17.6	49.3
	2	1.2	13.7	1.3	8.2
	3+	0.0	2.0	0.0	0.5
20 kph	0	1.4	0.0	28.9	2.7
	1	22.8	3.0	42.8	25.4
	2	37.5	15.4	22.7	42.4
	3+	38.3	81.5	5.6	29.5
25 kph	0	0.0	0.0	0.8	0.0
	1	0.0	0.0	7.0	0.0
	2	0.3	0.0	21.6	1.0
	3+	99.7	100.0	70.6	99.0

3.5 Tibia shaft injury

The risk of injury to the tibia shaft for female and male HBM is generally low at speeds below 30 kph but increases rapidly at speeds above 30 kph, please see Additional file 1: Figure S13 and S14. For the improved tram front both the female and the male HBM show for both impact locations a very low risk (< 15%) for a tibia shaft injury. The simulation results for the impact scenarios at 60 kph show some assessment irregularities and are therefore not included.

3.6 Lateral deflection

From 20 kph on, lateral deflections of more than 800 mm are achieved, i.e. the suggested limit for safety against being overrun is easily reached in all considered cases in accordance with CEN/TR 17420 [32], please see Additional file 1: Figure S8.

3.7 Holistic assessment of tram to pedestrian simulations

The generic improvement of the tram front leads to a decrease of all injury risks or shift towards lower injury severities for both, 50 M and 50F. For AIS 4 + concussions the risk was nearly halved as well as significant reduction for proximal femur (hip) and femur shaft fractures. For skull fractures, the risk was reduced by ~ 5% for 50F and 50 M. Also, for tibia fractures a significant reduction in the injury risk can be seen. The results are presented in Additional file 1: Table S3 and in form of individual graphs summarized in Additional file 1: Table S2.

4 Discussion

This study shows the beneficial application of virtual testing to analyses of tram-pedestrian accidents by application of HMBs: e.g., design variations, different anthropometries and impact speeds or locations, respectively, can be assessed easily. However, the difficulty in achieving safety improvements for a wider range of impact velocities also became evident. Further improvements require more sophisticated engineering solutions and eventually also active safety features such as front/window airbags.

The results show a significantly higher risk of severe head injury in the 25% lateral offset cases. This is due to the A-pillar that leads to a higher stiffness compared to the plain windscreen in the middle. On the other hand, the stiffness of the A-pillars must not be reduced due to structural crash safety requirements of the car body according to DIN EN 15227 [5]. But there is plenty of room for improvements by e.g. introducing softer outer A-pillar covers or modified windscreen-shapes for impacts close to the A-pillar. In general, the values for the HIC are much smaller compared to a previous study on tram-pedestrian accidents based on simulations with Madymo [34]. This is due to a deformable tram model including even windscreen glass failure used in the present study whereas the tram model of Weber et al. [34] is only a rigid body and the pedestrians are represented by ATDs instead of HBMs.

For a more conservative approach to the simulations, a linear elastic glass model without failure was also considered in a very specific speed range (25 to 35 kph). Since the relative impact velocities of the pedestrians' heads against the front windscreens are lower than the actual respective tram-pedestrian impact speed and the windshield of trams is required to provide a quite high ballistic resistance according to DIN EN 15152 [4] and UN/ECE [32], it is likely that the windshield will not break in this speed range and as a result the head is subjected to much higher forces/accelerations.

Overall, the HIC values remain below 1000 for impact speeds up to 25 kph (glass model without failure) and 35 kph (glass model with failure), respectively. The baseline tram front already complies with the geometric recommendations of CEN/TR 17420 [32] Therefore, the relatively low HIC result values in this velocity range can almost be considered as expected. Further evaluation of injuries shows that improvements of the tram front in terms of injury risk, e.g. risk for concussion (DAMAGE) or risk of femoral shaft fracture, obtained at 20 km/h are also beneficial at higher speeds. Due to the high severity of injury of certain body parts at speeds above 35 kph, passive safety measures no longer have a meaningful effect on most parts of the body.

It is an interesting result of this study that it does indeed show some gender specific results, e.g., the injury risks differ quite considerably in the centred impact case. The risk of diffuse brain injury for the female HBM in particular remains low in the range between 40 and 50 kph impact speeds onto the modified tram front, whereas the risk of focal injury estimated by the HIC increases almost linearly in this range but remains below the respective values for the baseline tram front. The modified version of the tram front shows a higher improvement for the female than for the male HBM in terms of HIC, but the opposite is the case for the evaluation of DAMAGE. At this point it is important to note that HIC is evaluated by linear acceleration and DAMAGE by rotational acceleration of the heads centre of gravity. For future investigations and standardization on this subject, respectively, it is strongly recommended to consider a wider range of HBMs (male, female and children).

The risk of injury to lower body regions, e.g., hip and femoral shaft, tends to be significantly higher for the female HBM than for the male HBM. These results are in very good agreement with the statistical data of Lackner et al. [18] on Swedish accident data that show a higher risk of abdominal and lower limb injuries for females. For the male HBM, the risk of proximal femur injury remains below 60% with the improved tram front at all speeds. This is partly due to the specific impact location of these body parts on the tram front, but also due to differences in bone dimensions and therefore resistance moments between female and male models. Much room is thus still left for improvements in geometric terms and also in the context of the tram nose softness to shift the average injury severity to higher speeds for the broadest range of vulnerable road users as possible.

Finally, the design goal of achieving a lateral deflection of pedestrians who have been hit with the objective of not having accident victim also run over by the tram is plausible on principle. Modern curved tram front designs also appear to be evolving towards reasonable lateral deflections in most cases anyway. However, another issue with higher impact speeds is the resulting large lateral HBM displacements which can lead to secondary collisions with arbitrary urban opponents, which can ultimately make accidents of this kind even more severe. It would also appear feasible to consider the kinematics in the x–z plane, which is deemed favourable if it directs the rebound of the struck pedestrian upwards. This helps to prevent the pedestrian from not to be knocked down to the ground in front of the tram's travel area.

4.1 Strengths and limitations

This is the first time that both a female and a male HBM are tested against the front mask of a rail vehicle, which demonstrates the differences in passive safety of public transport between a female vulnerable road user (VRU) and a male VRU.

The studied generic tram front follows the geometric guidelines of CEN/TR 17420 [32], which is intended to already provide a relatively pedestrian safe tram front design. It is assumed that the results presented in this work will reflect improvements that have already been implemented compared to typical trams of the past, which are currently still in service.

While the results based on accident statistics support the conclusions of this study, they must be considered carefully since a broader statistical basis is still desirable and in particular the impact speed probability evaluations also include assumptions for acceleration/deceleration.

Some simulations at lower speeds do not show head impacts onto the windscreen. This may be attributed in part to the fact that the VIVA model is currently relatively stiff in the shoulder area.

The GRP material of the tram's front skirts is modelled only by a linear elastic material card, so it is not certain whether the front skirts would show non-linear behaviour or even ruptures due to the impacts at higher speeds.

The glass model of the windscreen is developed according to data for 19 kph and 24 kph impacts, so it is currently not known whether the results for much higher or lower speeds are sufficiently reliable. The elastic glass model approach shows that it is very important to have an accurate glass model that correctly predicts failure. Furthermore, it is important to be aware of the critical (lower) impact speed that will in any case cause glass failure.

Finally, the results naturally reflect only the consequences of the primary impact between the HBM and the tram. It is not possible to cover the entire urban environment and all possible types of secondary impacts, although it is acknowledged that the secondary impact is not negligible [34].

5 Outlook

More comprehensive material modelling and validation is required to improve the prediction quality of virtual testing. At this point, it is particularly recommended that glass should be tested with the same dimensions used for the vehicle in question. For railway windscreens, European standards generally require safety glass for trams, which sometimes differ greatly in the number of layers used and the thickness of them. This should also be considered in the empirical tests as well as different impact velocities on the test specimens.

Since the front skirts also encounter the HBM during the primary impact, they should also be modelled with a validated material model, preferably with a non-linear material model that also takes damage into account. Here material modelling including tests is also highly recommended.

This paper shows that tram fronts can be improved with respect to pedestrian safety by the application of virtual testing, but the tram front design itself, however, offers only limited options especially regarding higher speeds. It is still worth exploiting these, however, to the greatest extent possible. Active safety such as driving assistance systems, e.g., automatic emergency braking (AEB) systems, should also be considered in addition to the passive measures, in order to decrease the impact speed of the tram or even avoid an accident. Nevertheless, the focus should never be solely on active systems, as these can fail, and the tram is unable to actively avoid pedestrians. Nevertheless, it is a critical accident partner due to its dimensions and mass. The combination of active and passive systems is thus desirable.

There is still a great scope for gaining deeper insights into tram pedestrians accidents, for instance regarding a broader variety of ages and body sizes that could influence injury risks and also including particular characteristics of tram related urban physical infrastructure.

Further investigations into future applications for accident avoidance in urban environments could be very helpful not only in the context of infrastructural measures such as barriers and visual or acoustic signals, respectively, but also with digital measures such as wearable alerting tools are imaginable for the future.

6 Conclusion

This study marks a starting point of HBM based virtual testing for tram-pedestrian incidents. The benefit of a softer tram front as a means of reducing injury severity was shown for two different HBMs representing the average female and male adult population. The baseline generic tram model follows geometric guidelines for tram front designs in the pedestrian safety context and the improved version of this tram front is in addition generically softened. The results show a relatively low risk of head injury at 20 kph for both tram fronts with respect to the HIC, but a significant risk of injury to the head with respect to DAMAGE. At this impact speed, the respective injury risk level of other body regions is already high but could be reduced by means of softening, e.g., it is possible that the femoral shaft values could even be halved. This is expected to also reduce the injury risks at higher speeds, but at speeds above 35 kph, however, injury indications generally point to multiple severe injuries for which survival is unlikely. By directly comparing female and male models, the differences in injury risk for different body regions, and how softening the tram front differentially reduces injury risk for specific body regions, it is shown that it is not sufficient to evaluate only a single adult anthropometry. It would therefore be very welcome if future standardization with respect to tram-pedestrian safety at least reflected on the admissibility of the use of virtual testing using HBMs for the assessment of new tram front designs.

Supplementary Information

The online version contains supplementary material available at https://doi.org/10.1186/s12544-023-00595-0.

Additional file 1. Supplementary material.

Author contributions

The main theme for this publication was developed and guided by CK and PH, respectively. CLa did most of the work regarding modelling, simulating and evaluating. The holistic assessment was compiled by CLe. All authors have read and approved the final manuscript.

Funding

This study has been conducted within the VIRTUAL project that has received funding from the European Union Horizon 2020 Research and Innovation Programme under Grant Agreement No. 768960.

Availability of data materials

The data analysed in this study is subject to the following licenses/restrictions: Raw data from numerical simulations are not publicly available. Requests to access these datasets should be directed to CL, and PH, respectively. The simulation setup, the VIVA + models and the generic tram front model are available on OpenVT.eu.

Declarations

Competing interests

Christian Lackner and Philipp Heinzl are employed by Siemens Mobility Austria GmbH. The remaining authors declare that the research was conducted in the absence of any commercial or financial relationships that could be construed as a potential conflict of interest.

Author details

[1]System Engineering, Siemens Mobility Austria GmbH, Leberstrasse 34, Vienna, Austria. [2]Vehicle Safety Institute, Graz University of Technology, Inffeldgasse 23, 8010 Graz, Austria.

Received: 24 November 2022 Accepted: 16 July 2023

References

1. AAAM. (2005). Abbreviated injury scale 2005. Des Plaines IL.
2. Bützer, D. (2022). Cost-benefit analysis of innovative automotive safety systems, Deliverable 6.1 of the H2020 project VIRTUAL.
3. Cho, J. R., Park, S. B., Ryu, S. H., Kim, S. H., & Lee, S. B. (2009). Landing impact analysis of sports shoes using 3-D coupled foot-shoe finite element model. *Journal of Mechanical Science and Technology, 23*, 2583–2591.
4. DIN EN 15152. (2019). Bahnanwendungen—Frontscheiben für Schienenfahrzeuge. Technisches Komitee CEN/TC 256. August, 2019.
5. DIN EN 15227. (2020). Bahnanwendungen – Anforderungen an die Kollisionssicherheit von Schienenfahrzeugen. Technisches Komitee CEN/TC 256. April, 2020
6. Euro NCAP. (2019). Pedestrian human model certification. (TB 024). https://cdn.euroncap.com/media/56949/tb-024-pedestrian-human-model-certification-v20.pdf
7. Euro NCAP. (2021): Pedestrian human model certification. (TB 024). - v3.0.1. November 2021.
8. Euro NCAP. (2023). Brain Injury Calculation. (TB 035). https://cdn.euroncap.com/media/77157/tb-035-brain-injury-calculation-v101.pdf
9. Forman, J. L., Kent, R. W., Mroz, K., Pipkorn, B., Bostrom, O., & Segui-Gomez, M. (2012). Predicting rib fracture risk with whole-body finite element models: Development and preliminary evaluation of a probabilistic analytical framework. *Annals of Advances in Automotive Medicine, 56*, 109–124.
10. Forman, J. L., Joodaki, H., Forghani, A., Riley, P., Bollapragada, V., Lessley, D., & Crandall, J. (2015). Biofidelity corridors for whole-body pedestrian impact with a generic buck. In *Proceedings of IRCOBI conference, ed. international research council on the biomechanics of injury (IRCOBI), 2015, Lyon, France*.
11. Gabler, L. F., Crandall, J. R., & Panzer, M. B. (2019). Development of a second-order system for rapid estimation of maximum brain strain. *Annals of Biomedical Engineering, 47*(9), 1971–1981. https://doi.org/10.1007/s10439-018-02179-9
12. Glansegg, B. (2016). Geschwindigkeitsprofil der Straßenbahnlinie 2. Bachelor Thesis. Institut für Verkehrswissenschaften. TU Wien. Vienna, Austria
13. Jezdik, R., Konopík, P., Rund, M., Svoboda, M., & Jelen, K. (2019). Aspect of front end tram design with respect to pedestrian safety. In *12th International symposium on passive safety of rail vehicles*, Prague, Czech Republic.
14. John, J., Klug, C., Kranjec, M., Svenning, E., & Iraeus, J. (2022). Hello, world! VIVA+: A human body model lineup to evaluate sex-differences in crash protection. *Frontiers in Bioengineering and Biotechnology, 10*, 918904. https://doi.org/10.3389/fbioe.2022.918904
15. Klug, C., Feist, F., Raffler, M., Sinz, W., Petit, P., Ellway, J., & van Ratingen, M. (2017). Development of a procedure to compare kinematics of human body models for pedestrian simulations. In *2017 IRCOBI conference proceedings* (pp. 508–530). International Research Council on the Biomechanics of Injury (IRCOBI).
16. Klug, C., Feist, F., Schneider, B., Sinz, W., Ellway, J., & van Ratingen, M. (2019). Development of a certification procedure for numerical pedestrian models. Paper Number 19-0310. In *26th International technical conference and exhibition on the enhanced safety of vehicles (ESV): Technology: Enabling safer tomorrow*. Eindhoven, Netherlands.
17. Kuntsche, J. (2015). *Mechanisches Verhalten von Verbundglas unter zeitabhängiger Belastung und Explosionsbeanspruchung* (p. 131). Springer.
18. Lackner, C., Heinzl, P., Rizzi, M. C., Leo, C., Schachner, M., Pokorny, P., & Klug, C. (2022). Tram to pedestrian collisions—Priorities and potentials. *Frontiers in Future Transportation, 3*, 877. https://doi.org/10.3389/ffutr.2022.913887
19. Larsson, K. J., Blennow, A., Iraeus, J., Pipkorn, B., & Lubbe, N. (2021). Rib cortical bone fracture risk as a function of age and rib strain: Updated injury prediction using finite element human body models. *Frontiers in Bioengineering and Biotechnology, 24*(9), 677768. https://doi.org/10.3389/fbioe.2021.677768.
20. Leo, C., Klug, C., Ohlin, M., & Linder, A. (2019). Analysis of pedestrian injuries in pedestrian-car collisions with focus on age and gender. In *2019 IRCOBI conference proceedings* (pp. 256–257). International Research Council on the Biomechanics of Injury (IRCOBI).
21. Linder, A., Bützer, D., Keller, A., Klug, C., Wijnen, W., & Schmitt, K. U. (2022). Open-source tools for road user safety assessment from the VIRTUAL project. In *Transport research arena (TRA) conference*.
22. Livermore Software Technology (LST). (2020). LS-DYNA keyword user's manual. In *VOLUME II material models*, Livermore, California.
23. Mohagheghian, I., Wang, Y., Zhou, J., Yu, L., Guo, X., Yan, Y., & Dear, J. P. (2017). Deformation and damage mechanisms of laminated glass windows subjected to high velocity soft impact. *International Journal of Solids and Structures, 109*, 46–62. https://doi.org/10.1016/j.ijsolstr.2017.01.006

24. Newman, J. (1986). A generalized acceleration model for brain injury threshold (GAMBIT). In *Proceedings of the 1986 international IRCOBI conference on the biomechanics of impact*. Zurich, Switzerland.
25. Sagberg, F., & Sætermo I. E. (1997). Traffic safety of tram transport. TØI report 367. https://www.toi.no/getfile.php/138906-1208933888/Publikasjoner/T%C3%98I%20rapporter/1997/367-1997/sum-367-97.pdf. Accessed 9 Feb 2022.
26. Schmitt, K. U., Niederer, P. F., Cronin, D. S., Morrison III, B., Muser, M. H., & Walz, F (2019). Trauma biomechanics: An introduction to injury biomechanics, 5th edn. In *Springer eBook collection*. Springer. https://doi.org/10.1007/978-3-030-11659-0
27. Schubert, A., Erlinger, N., Leo, C., Iraeus, J., John, J., & Klug, C. (2021). Development of a 50th percentile female femur model. In *IRCOBI conference proceedings* (pp. 308–332). IRCOBI. http://www.ircobi.org/wordpress/downloads/irc21/pdf-files/2138.pdf
28. Siemens, A. G. (2013). Straßenbahnsystem—ULF Wien, Österreich. Infrastructure & Cities Sector Rail Systems Division, Berlin, Germany.
29. Subit, D., Kerrigan, J., Crandall, J., Fukuyama, K., Yamazaki, K., Kamiji, K., & Yasuki, T. (2008). Pedestrian-vehicle interaction: Kinematics and injury analysis of four full-scale tests. In *Proceedings of IRCOBI conference, 2008, Bern, Switzerland*.
30. Takhounts, E. (2013). Development of brain injury criteria (BrIC). *Stapp Car Crash Journal*, *57*.
31. Technical Committee CEN/TC. (2019). *Railway applications—Vehicle end design for trams and light rail vehicles with respect to pedestrian safety* (p. 30). European Committee for Standardization.
32. UN/ECE. (2013). Uniform provisions concerning the approval of safety glazing materials and their installation on vehicles. Regulation No 43. Economic Commission for Europe of the United Nations. November 2013.
33. Watanabe, R., Miyazaki, H., Kitagawa, Y., & Yasuki, T. (2011). Research of the relationship of pedestrian injury to collision speed, car-type, impact location and pedestrian sizes using human FE model (THUMS Version 4). In *Proceedings of international technical conference on the enhanced safety of vehicles, 2011*, Washington, D.C., USA.
34. Weber, T., Muser, M., & Schmitt, K. U. (2015). Optimising the design of tramways to mitigate injury risk in pedestrian impacts. In *2015 IRCOBI conference proceedings* (pp. 339–349). International Research Council on the Biomechanics of Injury (IRCOBI).
35. Wiener, L. (2020). Betriebsangaben 2019. https://www.wienerlinien.at/media/files/2020/wl_betriebsangaben_2019_deutsch_358274.pdf. Accessed 21 February 2022.
36. Wu, T., Sato, F., Antona-Makoshi, J., Gabler, L. F., Giudice, J. S., Alshareef, A., & Panzer, M. B. (2022). Integrating human and nonhuman primate data to estimate human tolerances for traumatic brain injury. *Journal of Biomechanical Engineering*. https://doi.org/10.1115/1.4053209
37. Zhang, X., Hao, H., & Shi, Y. (2015). *The mechanical properties of polyvinyl butyral (PVB) at high strain rates* (p. 40). University of Western Australia.

Publisher's Note